Mixing Free Energy and Molecular Dynamics Simulations

Naoko NAKAGAWA and Akira YOSHIDA
Department of Physics, Ibaraki University
2-1-1 Bunkyo, Mito, Ibaraki 310-8512

1 Introduction

Mixing free energy determines the properties of a solution, while theories for its estimation are limited to rather dilute solutions [1, 2, 3]. A simpler numerical method applicable to the general mole fraction and valid regardless of the system size would be valuable. Alchemical free energy calculation is one of the free energy calculation methods often used in the numerical study of drug discovery [4, 5, 6, 7, 8, 9, 10, 11, 12, 13]. Extending the idea, we create a solution from a pure substance, which may provide a formula for calculating the mixing free energy. We thus propose a method for molecular dynamics simulations that estimates the mixing free energy. The details of the derivation and numerical confirmations are in the reference [14].

2 Mixing free energy and activity coefficients

The important quantity that determines the thermodynamic properties for the mixture is the mixing free energy $\Delta_{\rm mix}G$. This corresponds to the work required for quasistatic mixing at constant temperature and constant pressure, which is the sum of the enthalpy change in mixing and the mixing entropy $\Delta_{\rm mix}S$. The change in the thermodynamic properties of each substance is represented by excess chemical potential; i.e., the deviation of chemical potential from that of each pure substance. The excess chemical potential is written as

$$\beta\mu_{\rm A}^{\rm ex}(T,p,c) = \ln c + \ln\gamma_{\rm A}, \tag{1}$$
$$\beta\mu_{\rm B}^{\rm ex}(T,p,c) = \ln(1-c) + \ln\gamma_{\rm B}, \tag{2}$$

with the activity coefficients $\gamma_{\rm A}(T,p,c)$ and $\gamma_{\rm B}(T,p,c)$. c is the mole fraction in the mixture. The mixing Gibbs free energy is given by $\Delta_{\rm mix}G = N[c\mu_{\rm A}^{\rm ex} + (1-c)\mu_{\rm B}^{\rm ex}]$, where N is the total amount of molecules. When $\gamma_{\rm A} = \gamma_{\rm B} = 1$, the mixture is ideal; i.e., a molecule of substance A does not interact with a molecule of B. Then, $\Delta_{\rm mix}G^{\rm id} = -T\Delta_{\rm mix}S^{\rm id}$ with

$$\Delta_{\rm mix}S^{\rm id} = N[c\ln c + (1-c)\ln(1-c)]. \tag{3}$$

The activity coefficients $\gamma_{\rm A}$ and $\gamma_{\rm B}$ represent the intrinsic properties of the mixture that result from the interaction of the two pure substances. Determining $\Delta_{\rm mix}G$ identifies such intrinsic properties as

$$\Delta_{\rm mix}G + T\Delta_{\rm mix}S^{\rm id} = N[c\ln\gamma_{\rm A} + (1-c)\ln\gamma_{\rm B}], \tag{4}$$

because the ideal entropic effects $T\Delta_{\rm mix}S^{\rm id}$ has already known as (3).

3 Difficulty of numerical determination

In textbooks on thermodynamics [15, 16], a standard protocol for determining $\Delta_{\rm mix}S$ and $\Delta_{\rm mix}G$ for two pure substances is the quasistatic shift of two semi-permeable membranes

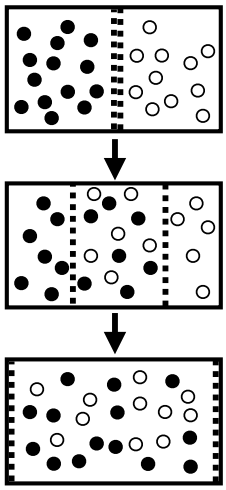

Figure 1: Quasi-static mixing process using two permeable membranes.

as shown in Fig. 1. Initially, two substances are spatially separated by two semi-permeable membranes. Then, shift the two membranes slowly enough as it is regarded as quasi-static. When each membrane reaches the left or right boundary wall, the container is filled with a mixture of the two substances.

We emphasize that this mixing process is difficult in computation involving huge computational resources. The speed of the shift of the membranes should be much slower than the velocity of molecules, as the process needs to be performed quasi-statically. Moreover, because the distance between each membrane and boundary wall is macroscopic, the process requires at least $O(N)$ time steps per trajectory. Thus, this number could be more such as $O(N^2)$. Such a high-cost calculation is hard to complete with a large enough system, and this is likely the reason that such processes are not usually used in the numerical investigation of the mixing entropy.

4 Work relation for determining mixing free energy

We consider microscopic operations called alchemical processes, which change the attributes, such as mass and size, of molecules. Alchemical methods are usually used to estimate the effect of substituting some groups into a large single molecule [6, 7]. We note that an alchemical method itself is not necessarily limited to single molecules but can be applied to multi-molecule systems to create a mixture from a pure substance. Below, we set alchemical protocols for creating a mixture taking care of the distinguishability of the molecules of the same species. Using the protocols we formulate the relation useful for the numerical determination of mixing free energy.

4.1 Setup

We deal with classical systems of N molecules packed in a cobid of volume V. The surrounding environment is at a constant temperature T. We write the Hamiltonian of the system as

$$H(\Gamma;\boldsymbol{\alpha}) = \sum_{i=1}^{N} \frac{\boldsymbol{p}_i^2}{2m_i} + \Phi(\{\boldsymbol{r}_i\};\boldsymbol{\alpha}_\Phi), \qquad (5)$$

where $\Gamma = (\{\boldsymbol{r}_i\},\{\boldsymbol{p}_i\})$ with the position $\boldsymbol{r}_i$ and momentum $\boldsymbol{p}_i$ for the ith molecule, and $(\{a_i\})$ is an abbreviation of $(a_1, a_2, \cdots, a_N)$. m_i is the mass of the ith molecule and the potential Φ comprises the interaction among molecules and the interaction between molecules and walls of the container, which are parameterized by the set $\boldsymbol{\alpha}_\Phi$. The whole of the opearational parameters are $\boldsymbol{\alpha} = (\{m_i\}, \boldsymbol{\alpha}_\Phi)$.

For investigating fixed pressure systems, we replace the Hamiltonian as

$$H_p(\Gamma, V;\boldsymbol{\alpha}) = H(\Gamma;\boldsymbol{\alpha}) + pV, \qquad (6)$$

by replacing a certain wall of the container with a movable wall at a constant pressure of p.

Suppose that an external operator changes the value of $\boldsymbol{\alpha}$ in the period $0 \le t \le \tau$. For

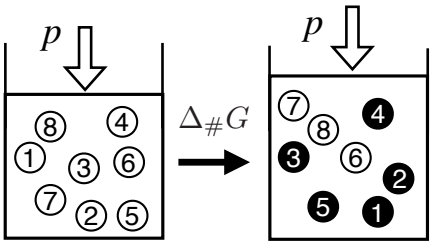

Figure 2: Alchemical processes for determining $\Delta_{\#}G$. The first n particles are changed from a species A to another species B.

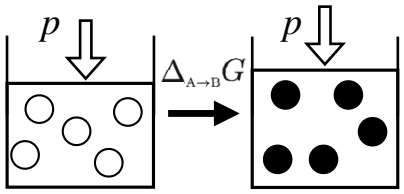

Figure 3: Alchemical processes for determining $\Delta_{\mathrm{A}\to\mathrm{B}}G$. All n particles are changed from a species A to another species B.

a protocol $\hat{\boldsymbol{\alpha}} = (\boldsymbol{\alpha}(t))_{t\in[0,\tau]}$, where $\boldsymbol{\alpha}_0 = \boldsymbol{\alpha}(0)$ and $\boldsymbol{\alpha}_1 = \boldsymbol{\alpha}(\tau)$, the work done by the external operator is written as

$$\hat{W}(\hat{\Gamma}) = \int_0^\tau ds\ \frac{d\boldsymbol{\alpha}}{ds}\cdot\left.\frac{\partial H(\Gamma(s);\boldsymbol{\alpha})}{\partial\boldsymbol{\alpha}}\right|_{\boldsymbol{\alpha}=\boldsymbol{\alpha}(s)}, \tag{7}$$

where $\hat{\Gamma} = (\Gamma(t))_{t\in[0,\tau]}$ is a trajectory in the phase space. We assume below that the system is in equilibrium at $\boldsymbol{\alpha}_0$ for $t \le 0$. For constant pressure systems, the volume V becomes a microscopic variable, and a trajectory in phase space is replaced by $(\hat{\Gamma}, \hat{V}) = (\Gamma(t), V(t))_{t\in[0,\tau]}$.

4.2 Alchemical protocols

We concentrate on a mixture of two species A and B, whose numbers of molecules are n and $N-n$, respectively. The mole fraction is $c \equiv n/N$.

We put N molecules of species A in a container and index all N molecules in order. After relaxing the system to equilibrium, we change the attributes of the first n molecules, $1 \le i \le n$, alchemically as they become another species B as depicted in Fig. 2. We write the work for completing the alchemical process as $\hat{W}_{\#}(\hat{\Gamma}, \hat{V})$. The resulting system is similar to a typical two-component mixture except that all molecules are indexed.

Let $G_{\mathrm{AB}^{\#}}$ be the free energy for the mixture of the indexed molecules, while G_{AB} be that for the usual mixture. We note that

$$G_{\mathrm{AB}}(T,p,n,N-n) \neq G_{\mathrm{AB}^{\#}}(T,p,n,N-n), \tag{8}$$

because the molecules are indexed. We can determine the difference from the pure substance A by measuring the work $\hat{W}_{\#}$ as

$$\begin{aligned}\Delta_{\#}G &\equiv G_{\mathrm{AB}^{\#}}(T,V,n,N-n) - G_{\mathrm{A}}(T,V,N),\\ &= -k_{\mathrm{B}}T\ln\left\langle e^{-\beta\hat{W}_{\#}}\right\rangle\end{aligned} \tag{9}$$

where $\langle\cdot\rangle$ is the average over trajectories $(\hat{\Gamma}, \hat{V})$.

We are also possible to determine the Gibbs free energy difference between the pure substances of A and B

$$\begin{aligned}\Delta_{\mathrm{A}\to\mathrm{B}}G &\equiv G_{\mathrm{B}}(T,V,n) - G_{\mathrm{A}}(T,V,n)\\ &= -k_{\mathrm{B}}T\ln\left\langle e^{-\beta\hat{W}_{\mathrm{A}\to\mathrm{B}}}\right\rangle,\end{aligned} \tag{10}$$

with the work in the alchemical process changing all n molecules from A into B as shown in Fig. 3.

4.3 Formula for the mixing Gibbs free energy

We have shown in [14] that the mixing free energy satisfies

$$\begin{aligned}\Delta_{\mathrm{mix}}G + T\Delta_{\mathrm{mix}}S^{\mathrm{id}} &= \Delta_{\#}G - \Delta_{\mathrm{A}\to\mathrm{B}}G\\ &= -k_{\mathrm{B}}T\ln\frac{\left\langle e^{-\beta\hat{W}_{\#}}\right\rangle}{\left\langle e^{-\beta\hat{W}_{\mathrm{A}\to\mathrm{B}}}\right\rangle}\end{aligned} \tag{11}$$

with errors smaller than $\ln N$. We emphasize that $\Delta_{\mathrm{mix}}G$ in (11) is determined just from two alchemical processes in Fig. 2 and Fig. 3.

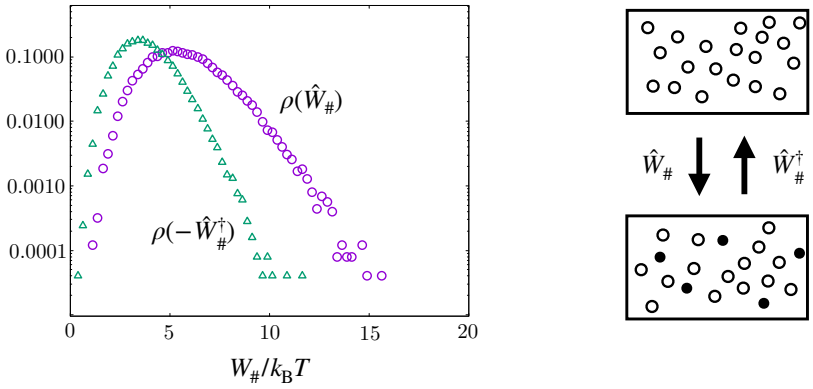

Figure 4: Work distributions in the left figure for the forward and backward protocols for creating a mixture. Here, operation time is $1000\tau_{\rm MD}$. The shape of the distribution depends on the operation time. The sketch of the protocols is shown in the right figures.

process	operation time
textbook	30000 $\tau_{\rm MD}$
A $\to$ B	400 $\tau_{\rm MD}$
#	400 $\tau_{\rm MD}$

Table 1: Comparison of operation times for calculating $\Delta_{\rm mix}G$ for the mixture of two substances of mass m and $2m$ with $c = 0.5$.

process	operation time
textbook	15000 $\tau_{\rm MD}$
A $\to$ B	2050 $\tau_{\rm MD}$
#	2050 $\tau_{\rm MD}$

Table 2: Comparison of operation times for calculating $\Delta_{\rm mix}G$ for the mixture of two substances of diameter σ and 2σ with $c = 0.5$.

The estimates of activity coefficients are a major issue in the research of mixtures, especially from the point of chemical engineering. The relation (11) may offer a new method of estimating the activity coefficients for various mixtures and solutions, which involves only a molecular dynamics simulation with two types of the alchemical process. Moreover, (11) can be applicable not only to dilute mixtures but rather to the mixture showing unstable and dynamic collective behaviors appeared in the first-order transitions. The formula (11) provides a general work relation giving the mixing free energy $\Delta_{\rm mix}G$ at constant pressure.

4.4 Advantage of (11) for numerical determination of $\Delta_{\rm mix}G$.

Compared with the mixing free energy calculation along the standard textbook process in Fig. 1, the numerical cost to calculate (11) is not expensive. We show comparison examples for the calculation costs in Tables 1 and 2 provided in constant temperature and volume. The first example is the mixture of two isotopes whose components differ only in mass. The computation time for completing the process in Fig. 1 takes about 37 times longer than the sum of the computation times for the alchemical processes in Fig. 2 and Fig. 3. In the second example, two components are different in size. The computation time required for the two alchemical processes is about 25% of the time for the textbook process in Fig. 1.

We show the work distribution $\rho(\hat{W}_\#)$ and $\rho(-\hat{W}^\dagger_\#)$ for the second example. Here, $\hat{W}_\#$ is the work measured in the alchemical process from the pure substance to a mixture, while $\hat{W}^\dagger_\#$ is the work for the backward protocol for creating the pure substance from the mixture. We find a cross point of the two dis-

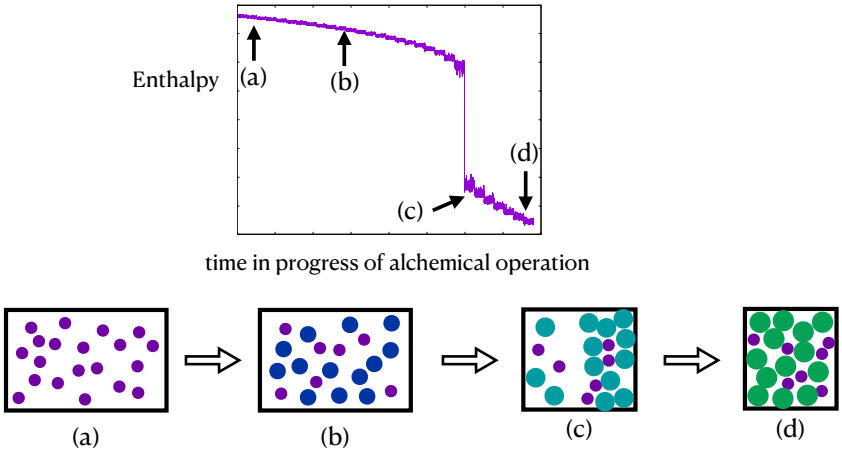

Figure 5: (a)(b)(c)(d) Schematic snapshots during the protocol from (a) an initial pure argon gas state to (b) the final target mixture of argon and krypton. Each argon molecule is depicted by a purple circle and each krypton molecule by a green circle. The other colored circles represent intermediate hypothetical molecules existing during the alchemical process. (Top) Time evolution of enthalpy during the process from (a) to (d). The jump in enthalpy suggests a transition from gas to liquid.

tributions, which confirms the convergence of the free energy difference $\Delta_{\#}F$. We check such work distributions for various operation times. We then determine the operation time for obtaining plausible free energy difference, which are depicted in Tables 1 and 2.

In the above examples, we took constant volume conditions. This is an essential point for the computation. The two alchemical processes in Fig. 2 and Fig. 3 are well-defined in constant pressure protocols while the mixing process with two semi-permeable membranes in Fig. 1 cannot be performed quasi-statically while keeping constant pressure. This is due to the osmotic pressure. Once the mid-region surrounded by the two semi-permeable membranes appears, all molecules tend to flow into the mid-region.

5 Example of a dense mixture with a first-order transition

We present an example of $\Delta_{\mathrm{mix}}G$ determined from the molecular dynamics simulation for a mixture of argon and krypton at constant temperature and constant pressure. The mixture is modeled as three-dimensional Lennard–Jones liquids. We use the LAMMPS package in this demonstration. The molecules are packed in a cuboid whose volume can fluctuate while keeping an aspect ratio of $21:5:5$ to fix the value of pressure. The container is periodic in y and z directions whereas two boundary walls are set perpendicularly to the x axis.

In detail, the interaction of any two molecules, argon or krypton, is given by the Lennard–Jones potential,

$$\phi(r;\epsilon,\sigma) = 4\epsilon\left[\left(\frac{\sigma}{r}\right)^{12} - \left(\frac{\sigma}{r}\right)^{6}\right], \qquad (12)$$

with a cutoff length $r_{\mathrm{c}} = 3\sigma_{\mathrm{Kr}}$. For the argon pair, $\sigma_{\mathrm{Ar}} = 3.401\,\text{Å}$ and $\epsilon_{\mathrm{Ar}} = 0.2321\,\mathrm{kcal/mol}$, whereas $\sigma_{\mathrm{Kr}} = 3.601\,\text{Å}$, $\epsilon_{\mathrm{Kr}} = 0.3270\,\mathrm{kcal/mol}$ for the krypton pair [17]. For the pair of argon and krypton, $\sigma_{\mathrm{ArKr}} = (\sigma_{\mathrm{Ar}} + \sigma_{\mathrm{Kr}})/2 = 3.501\,\text{Å}$ and $\epsilon_{\mathrm{ArKr}} = \sqrt{\epsilon_{\mathrm{Ar}}\epsilon_{\mathrm{Kr}}} = 0.2755\,\mathrm{kcal/mol}$ according to the Lorentz–Berthelot law [18, 19]. The masses of argon and krypton are $m_{\mathrm{Ar}} = 39.95\,\mathrm{g/mol}$ and $m_{\mathrm{Kr}} = 83.80\,\mathrm{g/mol}$. We perform the molecular dynamics simulations of

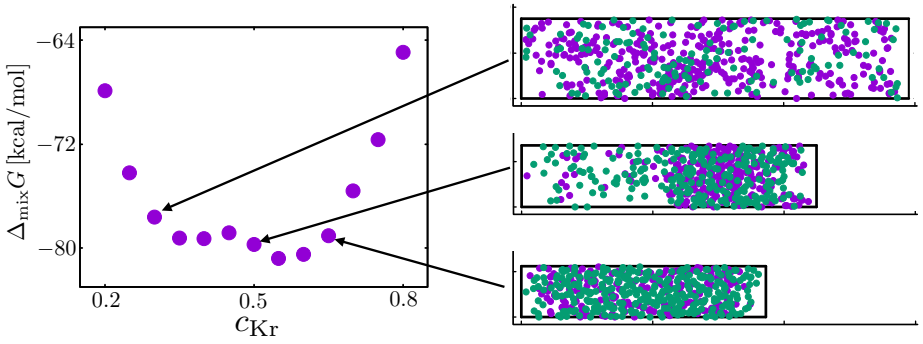

Figure 6: (Left) $\Delta_{\mathrm{mix}}G$ for the binary mixture of argon and krypton with $N = 500$ determined using (11). (Right) Snapshots of the particle distribution for the mixture of argon (purple) and krypton (green) for $c_{\mathrm{Kr}} = 0.3$, 0.5, and 0.65. The three-dimensional space is projected onto the two-dimensional space. The original figures are Figs. 7 and 9 in reference [14].

the constant temperature and pressure in $T = 163.15\,\mathrm{K}$ and $p = 4\,\mathrm{MPa}$ by adopting the Nose–Hoover chain and Martyna–Tobias–Klein barostat [20].

Liquid–vapor transition is observed with an increasing molar fraction $c_{\mathrm{Kr}} = N_{\mathrm{Kr}}/N$ of the krypton [21]. The right figures in Fig. 6 show snapshots of the system's configuration in $N = 500$ after sufficient relaxation for $c_{\mathrm{Kr}} = 0.3$, 0.5, and 0.65. The volume differs greatly among the three values of c_{Kr}. The number density at $c_{\mathrm{Kr}} = 0.65$ is approximately 5 times that at $c_{\mathrm{Kr}} = 0.3$, and dense and dilute regions coexist at $c_{\mathrm{Kr}} = 0.5$. Such behaviors exhibit the characteristics of liquid–vapor transition. These observations are consistent with the previous report in [21].

The alchemical protocol for calculating $\Delta_{\#}G$ is designed as follows: We take the initial pure substance as being argon in Fig. 5(a). Then, change the value of (m, σ, ϵ) related to the first n molecules from those of argon to krypton gradually in time. The snapshots of the system may be observed as Fig. 5(b) and (c). Here, the molecules during the protocol are hypothetical, not argon or krypton. Even in a single trajectory, we observe a sudden decrease in enthalpy and volume as shown in Fig. 5. The equilibrium state for the hypothetical system changes to liquid as shown in Fig. 5(d).

Calculating both $\Delta_{\#}G$ and $\Delta_{\mathrm{Ar}\to\mathrm{Kr}}G$, the resulting mixing free energy $\Delta_{\mathrm{mix}}G$ is shown in Fig. 6 for $N = 500$. The curve has a double-well shape and is convex upwards in the approximate range of $0.35 < c_{\mathrm{Kr}} < 0.55$ showing the liquid–vapor coexistence. We thus conclude that the functional shape of $\Delta_{\mathrm{mix}}G$ well characterizes the liquid–vapor transition for the argon–krypton mixture. Our formula (11) works as a quantitative method for determining the mixing Gibbs free energy.

The main term of the finite-size effects is of $\ln N$, which is about 1% of N at $N = 500$. This may affect thermodynamic properties. Indeed, the upward convexity in $\Delta_{\mathrm{mix}}G$ is not expected in the thermodynamic limit. To examine the system size dependence of $\Delta_{\mathrm{mix}}G$, we have performed the same calculations for $N = 4,000$ and $N = 13,000$. As the system size becomes larger, we find longer relaxation time. Especially when the trajectory passes through a transition from gas to liquid or from liquid to gas as demonstrated in Fig. 5, the relaxation time becomes significantly longer.

In the present temperature and pressure, the pure argon behaves as gas while the pure krypton does as liquid. Depending on the mole

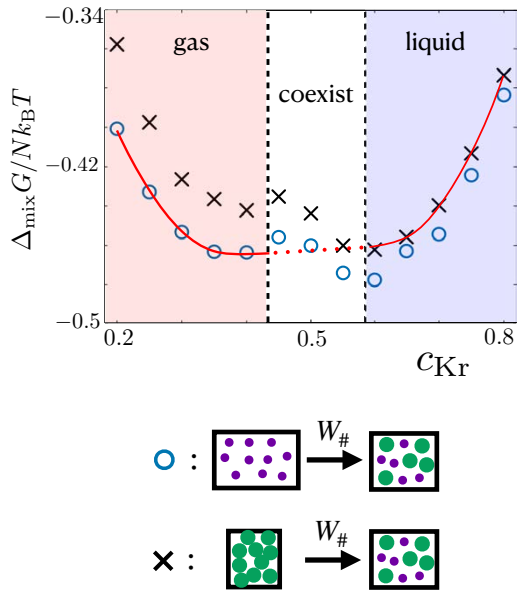

Figure 7: $\Delta_{\rm mix}G$ for the binary mixture of argon and krypton with $N = 4,000$ determined using (11). The circle points are calculated adopting the initial pure material as argon gas, whereas the initial pure material is chosen as krypton liquid in the cross points.

fraction $c_{\rm Kr}$ of the target mixture, the final state is different, i.e., gas, liquid, or liquid-gas coexistence. Suppose we choose the initial pure material as krypton when the target mixture is gas. Each trajectory shows a transition from liquid to gas as in Fig. 5, which may induce hysteresis. This transition may depend on the trajectory and is likely to show hysteresis. Then, the calculated results may not belong to equilibrium properties. To examine such a possibility, we compare two initial conditions; one starts from the pure argon and the other is from the pure krypton. The former is from gas and the latter is from liquid. As shown in Fig. 7, the obtained $\Delta_{\rm mix}G$ depends on the initial condition in $N = 4,000$.

Such differences do not appear in $N = 500$. This is because the fluctuations seem large enough to pass all typical equilibrium configurations when $N = 500$. By choosing the initial pure material properly, i.e., as the initial material is in the same phase as the target mixture, we avoid the difficulty due to the hysteresis. The red line in Fig.7 is drawn by choosing the results without experiencing transition. Comparing with Fig. 6, we find that $\Delta_{\rm mix}G$ in small $c_{\rm Kr}$ is slightly smaller with increasing N. As a result, the upward convexity seems to become flattened with increasing the system size N. The obtained $\Delta_{\rm mix}G$ would be reliable.

Acknowledgment

The present work was supported by KAKENHI (Nos. 17H01148, 19K03647, 20K20425). A. Y. was supported by JST and the Establishment of University Fellowships Towards the Creation of Science Technology Innovation under Grant Number JPMJFS2105. The numerical simulations in this work were done using the facilities of the Supercomputer Center, the Institute for Solid State Physics, The University of Tokyo.

References

[1] R. E. Skyner, J. L. McDonagh, C. R. Groom, T. Van Mourik, and J. B. O. Mitchell, A review of methods for the calculation of solution free energies and the modelling of systems in solution, Phys. Chem. Chem. Phys. **17**, 6174 (2015).

[2] M. Kohns, S. Reiser, M. Horsch, and H. Hasse, Solvent activity in electrolyte solutions from molecular simulation of the osmotic pressure, J. Chem. Phys. **144**, 084112 (2016).

[3] P. W. Debye and E. Huükel, Zur Theorie der Elektrolyte, Phys. Z. **24**, 185 (1923).

[4] C. Chipot and A. Pohorille (Eds.), *Free Energy Calculations: Theory and Applications in Chemistry and Biology*, Springer Series in Chemical Physics Vol. 86 (Springer-Verlag, Berlin, 2007).

[5] B. Cheng and M. Ceriotti, Computing the absolute Gibbs free energy in atomistic simulations: Applications to defects in solids, Phys. Rev. B **97**, 054102 (2018).

[6] P. Kollman, Free energy calculations: Applications to chemical and biochemical phenomena, Chem. Rev. **93**, 2395 (1993).

[7] P. A. Kollman, Advances and continuing challenges in achieving realistic and predictive simulations of the properties of organic and biological molecules, Acc. Chem. Res. **29**, 461 (1996).

[8] T. Simonson, G. Archontis, and M. Karplus, Free energy simulations come of age: Protein-ligand recognition, Acc. Chem. Res. **35**, 430 (2002).

[9] D. L. Mobley, J. D. Chodera, and K. A. Dill, On the use of orientational restraints and symmetry corrections in alchemical free energy calculations, J. Chem. Phys. **125**, 084902 (2006).

[10] D. L. Mobley and P. V. Klimovich, Perspective: Alchemical free energy calculations for drug discovery, J. Chem. Phys. **137**, 230901 (2012).

[11] T. Steinbrecher, C. Zhu, L. Wang, R. Abel, C. Negron, D. Pearlman, E. Feyfant, J. Duan, and W. Sherman, Predicting the effect of Amino Acid single-point mutations on protein stability-Large-scale validation of MD-based relative free energy calculations, J. Mol. Biol. **429**, 948 (2017).

[12] M. Kuhn, S. Firth-Clark, P. Tosco, A. S. J. S. Mey, M. MacKey, and J. Michel, Assessment of binding affinity via alchemical free-energy calculations, J. Chem. Inf. Model. **60**, 3120 (2020).

[13] J. Scheen, W. Wu, A. S. J. S. Mey, P. Tosco, M. Mackey, and J. Michel, Hybrid alchemical free energy/machine-Learning methodology for the computation of hydration free energies, J. Chem. Inf. Model. **60**, 5331 (2020).

[14] A. Yoshida and N. Nakagawa, Work relation for determining the mixing free energy of small scale mixtures, Phys. Rev. Res. **100**, 125125 (2022).

[15] J. W. Gibbs, On the equilibrium of heterogeneous substances, Trans. Conn. Acad. Arts Sci. **3**, 343 (1875-1878).

[16] E. Fermi, *Thermodynamics* (Dover, New York, 1956).

[17] S. K. Oh, Modified Lennard-Jones potentials with a reduced temperature-correction parameter for calculating thermodynamic and transport properties: Noble gases and their mixtures (He, Ne, Ar, Kr, and Xe), J. Thermodyn. **1**, 29 (2013).

[18] H. A. Lorentz, Ueber die Anwendung des Satzes vom Virial in der kinetischen Theorie der Gase, Ann. Phys. **248**, 127 (1881).

[19] D. Berthelot, Sur le mèlange des gaz, C. R. Acad. Sci. **126**, 1703 (1889).

[20] G. J. Martyna, D. J. Tobias, and M. L. Klein, Constant pressure molecular dynamics algorithms, J. Chem. Phys. **101**, 4177 (1994).

[21] A. E. Nasrabad, R. Laghaei, and U. K. Deiters, Prediction of the thermophysical properties of pure neon, pure argon, and the binary mixtures neon-argon and argon-krypton by Monte Carlo simulation using ab initio potentials, J. Chem. Phys. **121**, 6423 (2004).